Semiannual Progress Report

on work under

NASA-Ames Grant NSG2057

for the period

1 Dec. 1974 to 1 June 1975

A Sensitive Far Infrared Detection System

Roger H. Hildebrand
Principal Investigator
The Enrico Fermi Institute
The University of Chicago
Chicago, Il. 60637

NASA Technical Officer: R.M. Cameron, NASA-Ames Research Center

Semi Annual Progress Report

1 Dec. 1974 to 1 June 1975

During the first six months of our work with NASA support we have made observational tests of three prototype field optics systems of a novel design. The design concept and most of the laboratory tests were completed at the beginning of the grant period. The construction of prototypes and the execution of the observational tests occupied the period of this progress report.

The following manuscript, prepared for submission to Applied Optics describes the objectives, principles, and performance of the technique we have developed, and thus provides a comprehensive summary of our work up to 1 June 1975.

THE HEAT TRAP: AN OPTIMIZED FAR INFRARED FIELD OPTICS SYSTEM

D.A. Harper, R.H. Hildebrand, R. Stiening, and R. Winston

D.A. Harper is with the Department of Astronomy and Astrophysics, The University of Chicago, Yerkes Observatory, Williams Bay, Wisconsin, 53191. R.H. Hildebrand and R. Winston are with the Enrico Fermi Institute and the Department of Physics, The University of Chicago, Chicago, Illinois, 60637. R. Stiening is with the Fermi National Accelerator Laboratory, P.O. Box 500, Batavia, Illinois, 60510.

Abstract

An infrared field optics system has been designed which achieves the maximum flux concentration allowed by the Abbe sine inequality and provides efficient coupling to bolometer-type detectors.

I. Introduction

In far infrared astronomy the lower limit to the detectable radiant flux is determined, in many instances, by the intrinsic noise in the radiation detector. For the most sensitive detectors, currently liquid helium-cooled bolometers, the intrinsic noise increases with increasing detector size, and hence depends on the flux concentration which can be produced by the optical system. At wavelengths longer than about 200μm the detectable flux is further limited by the reduced absorptivity of the detector surface.[1] In this paper we describe the heat trap, a novel field optics system designed for maximum concentration and efficient reception of far infrared and submillimeter radiation.

The heat trap differs from conventional field optics in two respects. (1) The concentration of the incident radiation is produced by an ideal light collector[1-3] (focal ratio 1/2); not by a lens or by a spherical or parabolic mirror (minimum useful focal ratio ~1; see section IIC). (2) The radiation detector is placed in a cavity whose entrance coincides with the exit aperture of the light collector. When properly matched to the light collector, the cavity has the effect of increasing the absorptivity of the detector.

For detectors of a given size and applications in which sky noise, background noise, and background loading of the detector are negligible, the signal to noise ratio which can be achieved or extended sources with the heat trap can be more than four times larger than with conventional field optics. Alternatively, for a given field of view, the area of the detector can be reduced by a factor of four.

The components of the heat trap are represented schematically in Fig. 1. Beam patterns for three heat traps are shown in Fig. 2.

In the following sections we present certain general observations about field optics, and discuss the design, configuration, and performance of heat traps.

II. General Considerations in the Design of Field Optics

The principal functions of a field optics system are i) to distribute the energy from each image point uniformly across the detector, ii) to restrict the field of view of the detector to the image space of the telescope thereby reducing the reception of background radiation, and iii) to concentrate the radiation onto a detector smaller than the field aperture.

In this section we shall discuss the useful limits of flux concentration for various types of field optics under conditions frequently encountered in far infrared astronomy.

A. Assumed Conditions

1. We shall assume that the object to be examined is extended, or that it is to be viewed at wavelengths long compared to the dimensions of the smallest practical detector, or both. Under these conditions there will be an advantage in maximum flux concentration. (For point objects at short wavelengths one easily obtains images smaller than the smallest detectors. In that case no increase in detected flux can be gained by increased concentration.)

2. We shall further assume that the size of the detector must not be increased to compensate for abberations in the field optics. This consideration is important when a compact, well defined beam pattern is desired or when increasing the detector size would result in an increase in noise equivalent power.

3. Finally, we assume that it will often be necessary to limit the entrance aperture to the size of the diffraction disc of the telescope. This restriction implies an exit aperture comparable to the wavelength (see section II D), and hence introduces considerations of physical optics.

B. Flux Concentration, C

For a system without losses, the effective flux concentration, C, is given by

$$C = S_1/S_2 \tag{1}$$

where $S_1 = \pi r_1^2$ = area of entrance aperture and S_2 = area of exit aperture (πr_2^2) or irradiated area of bolometer, as may be appropriate. We assume that the detector is placed at the exit aperture or in a cavity of aperture S_2.

C. Limiting Values of C for Various Systems

1. Lenses

A field optics lens corrected for spherical aberration and coma will demagnify the exit pupil of the telescope according to the relationship

$$r_2/r_1 = f_F/f_T \tag{2}$$

where f_F = focal ratio of field optics and f_T = focal ratio of telescope.

The focal ratio of the telescope is related to the maximum angle, θ_T, of the rays in its image space by the expression[4]

$$f_T = 1/(2 \sin \theta_T). \tag{3}$$

Using (1), (2), and (3) we have

$$C = 1/(2f_F \sin \theta_T)^2. \qquad (4)$$

We emphasize that with focal ratios as commonly defined, expressions (2), (3), and (4) are valid only in the absence of spherical aberration and coma.

The lowest practical value for f_F is ~1. This is not a rigorous limit. For example, Des Cartes[5] and Huygens[6,7] have designed aspherical lens systems which are capable, in principle, of achieving the limit f = 0.5 imposed by the Abbe sine law. But, the performance of these and other low focal-ratio lens systems is severely limited by aberrations and, in many cases, by absorption losses. For systems to be used in infrared field optics it is realistic to assume $f_F \gtrsim 1$ and hence

$$C(\text{lens}) \lesssim 1/(4 \sin^2 \theta_T) \qquad (5)$$

Immersion systems, in which the detector is placed in optical contact with a medium of refractive index n, can enhance the flux concentration by a factor n^2. Whenever this technique is applicable, however, the same enhancement can be realized using a solid ideal light collector.[8]

2. Spherical or Parabolic Mirrors

Since bolometers are usually mounted in metal substrates which are large and opaque, they are most often placed off the axis of mirror systems. In principle, however, better light concentration can be achieved if the detector is on-axis directly in front of the field optics mirror.

We consider first a thin round detector on the mirror axis as shown in Fig. 3A. Since we wish to maximize C, we must find the value of ϕ which will minimize d_2/d_1 under the restriction (A2) that the system be efficient (i.e. that no rays striking the mirror at angles $\leq \theta_T$ miss the detector.)

Referring to the figure we see that the detector must be made large enough to intercept the divergent beam reflected from the edges of the field mirror. When this condition is met, the edges of the detector and field mirror lie on a common circle (radius r). Hence we have

$$d_1 = 2r \sin \phi$$

and

$$d_2 = 2r \sin 2\theta_T,$$

so that

$$d_2/d_1 = \sin 2\theta_T/\sin \phi. \qquad (6)$$

From Eq. 6, we see that d_2 will be minimized at $\phi = \pi/2$. With that value of ϕ expression (1) becomes

$$\begin{aligned} C \text{ (mirror, disc detector)} &= (d_1/d_2)^2 - 1 \\ &= (1/4 \sin^2 \theta_T)(\cos 2\theta_T/\cos \theta_T)^2 \\ &< 1/(4 \sin^2 \theta_T) \end{aligned} \qquad (7)$$

over the physical range of θ_T which lies in the interval $0 < \theta_T < \pi/4$. Notice that the expression (7) allows for blocking a portion of the incident beam corresponding to the detector area. We conclude that the concentration for the field mirror has the same limit as that for the lens (Eq. 5).

The analysis is readily extended to the case of a spherical detector of diameter $d_2 = 2\rho \sin \theta_T$ (See Fig. 3B). We now have $d_2/d_1 = \text{Sin } \theta_T/\text{Sin}(\phi/2)$ which is minimized at $\phi = \pi$. With that value of ϕ and with

$$S_1/S_2 = d_1^2/4d_2^2,$$

we have

$$C \text{ (mirror, spherical detector)} \leq 1/(4 \sin^2 \theta_T), \qquad (8)$$

again the same limit.

3. Ideal Light Collectors

The ideal light collector,[1-3] is a hollow, axially-symmetric, non-focussing light reflector. When used as the final resolution element properly matched to an imaging system (e.g., a telescope), it bestows upon the total system an effective focal ratio f = 0.5. A meridian section of the collector is shown in Figure 1. Light incident upon an entrance aperture of radius r_1 at an angle $\theta \leq \theta_1$ to the axis is channeled through an exit aperture of radius

$$r_2 = r_1 \sin \theta_1. \qquad (9)$$

This is the theoretical maximum concentration of a light beam with angular divergence θ_1 allowed by phase space conservation (the Abbe sine inequality).[3] The profile curve of the reflector is a parabola with focus at the opposite edge of the exit aperture and axis inclined at θ_1 with respect to the optic axis.[1,2] The resulting length of the collector is just sufficient to transmit direct rays at angle θ_1. The principle of the light collector is discussed in ref. 3.

To match the light collector to the telescope one chooses $\theta_1 = \theta_T$. Using (9) we have

$$C \text{ (ideal light collector)} = 1/\sin^2 \theta_T. \tag{10}$$

We conclude that the ideal light collector achieves a four-fold greater flux concentration than the lens or mirror systems discussed above [cf. eq'ns (5), (7), and (8)].

D. Considerations of Physical Optics: Efficiency at the Diffraction Limit

At the entrance aperture, the radius, δ, of the diffraction disc is given by

$$\delta = 1.22 \lambda f_T. \tag{11}$$

If we require that r_1 be no greater than δ then, using equation (2), we have

$$r_2 \leq 1.22 \lambda f_F. \tag{12}$$

If we further require that there be no serious losses due to diffraction effects within the field optics then there will also be some lower limit to the ratio $r_2/\lambda f_F$, and for any system one must demonstrate that the upper limit (to conserve resolution), and the lower limit (to conserve flux) are compatible; i.e., that the interval

$$K \lambda f_F \leq r_2 \leq 1.22 \lambda f_F \tag{13}$$

exists, where K is some minimum value of $r_2/\lambda f_F$ above which the efficiency is not appreciably diminished from its short wavelength value.

We shall not attempt to pursue this question analytically; instead we leave it as a matter for performance tests. (See section IVC).

III. Design Characteristics of the Heat Trap

Within the framework of geometrical optics it appears that an ideal light collector should offer a four-fold advantage in flux concentration over a conventional mirror or lens of optimum design (section IIC).

A further advantage in signal should be attainable by trapping the concentrated flux in a cavity such that radiation reflected by the detector surface has a high probability of being redirected toward the detector and a correspondingly low probability of escape from the cavity aperture.

In the heat trap an ideal light collector and a cavity are directly coupled to form a compact system which is easily aligned and well suited to arrangement in close-packed arrays (see section IIID). As we shall demonstrate (section IVC), the heat trap satisfies the condition of high efficiency at the diffraction limit [eq'n (13)].

A. Light Collector

As shown by comparison of Fig's 2C and 4, the beam pattern of a heat trap depends not only upon the characteristics of the condensing optics but also upon those of the cavity. In this section, however, we shall assume a perfect cavity and will discuss the inherent angular acceptance characteristics of the ideal light collector.

For meridional rays, the angular cut-off of a perfect collector (for $\lambda << r_2$) is discontinuous at $\theta = \theta_1$. The cut-off averaged over all rays occurs over a finite angular interval $\Delta\theta << \theta_1$. Specifically, defining $\Delta\theta$ to be the interval in which the intensity drops from 3/4 to 1/4 of its maximum value, we find by ray tracing that $\Delta\theta/\theta_1$, is a decreasing function of θ, as shown in Fig. 5. Within the accuracy of our computation the half width at half maximum is equal to θ_1.

To allow for effects of diffraction within the collector we assume that all the diffraction occurs at the entrance aperture. To allow for reflection losses we assume 5% absorption at each reflection. (Average number of reflections [<2] is slightly dependent on θ). For laboratory tests in which the beam pattern is measured by rotating the heat trap on a turntable only a meter or so from the radiation source, we fold in the angular spread due to the finite apertures of the source and collector.

We have calculated the dashed curves of Fig. 2 taking these various effects into account.

B. Cavity

We have designed the cavity empirically using a large optical model, and have found by subsequent tests (section IV) that the design is satisfactory at infrared wavelengths with the heat trap dimensions reduced sufficiently to satisfy the condition $r_1 \leq \delta$ (see section IID).

The model is shown schematically in Fig. 6. The entrance of the light collector is exposed to uniform illumination from the white-box. If all radiation entering within the desired acceptance cone is absorbed then none should re-emerge within that cone. Ideally, then, the photocell should read zero for all $\theta < \theta_1$.

In Fig. 7 we show examples of the "inverse" beam patterns obtained with the model. The curves for the cylindrical cavity show the effect of varying the distance, ℓ_B, from the cavity aperture to the bolometer surface.

If $\ell_B = 0$ then the cavity has no effect and the fraction of the radiation which is absorbed can be no larger than the absorptivity of the detector surface, (measurements made with gray bolometer). If $\ell_B = \ell_C$ (see Fig. 1) then no rays can reach the bottom surface and the ratio of effective sensor surface to cavity aperture is reduced from ~2 to ~1. The probability that a photon will be absorbed before having a chance to escape will be correspondingly reduced. The cavity is most effective for values of ℓ_B/ℓ_C in the range 0.3 to 0.4.

C. Summary of Heat Trap Proportions

The dimensions of a heat trap for a particular application are fixed by the choice of telescope and beam size.

The acceptance angle, θ_1, is matched to the focal ratio, f_T, of the telescope by the expression,

$$\theta_1 = \text{arc sin } (1/2f_T) . \tag{15}$$

The radius, r_1, of the entrance aperture is given by

$$r_1 = \theta_b f_T d_T \tag{16}$$

where θ_b is the angular radius of the desired field of view and d_T is the diameter of the telescope mirror.

Taking θ_1 [from eq'n (15)] and r_1 [from eq'n (16)] as initial parameters, we may fix the remaining dimensions (as defined in Fig.1) as follows:

$$d_2 = d_1 \sin \theta_1 \tag{17}$$

or

$$d_2 = d_1/2f_T, \tag{18}$$

$$\ell_L = (d_1 + d_2)/(2 \tan \theta_1) \tag{19}$$

or

$$\ell_L = d_2(2f_T + 1)\ (4f_T^{\ 2} - 1)^{1/2}/2, \tag{20}$$

$$d_B \simeq d_2, \tag{21}$$

$$d_C \leq 2d_B, \tag{22}$$

$$\ell_C \geq d_C, \tag{23}$$

and

$$\ell_B \simeq 0.35\ell_C \tag{24}$$

The detector leads enter the cavity through slots of width $w \ll d_C$. All reflecting surfaces of the funnel and cavity are gold plated.

D. Arrays

Heat traps have certain characteristics which should permit convenient arrangement in close-packed arrays. In particular, the detectors are on-axis behind the condensing optics, the alignment of the cavities is not critical, the light collectors are self-baffling, and the alignment of individual heat traps with respect to each other is almost automatic if the outside surfaces are straight cylinders.

IV. Performance Characteristics

In evaluating a system of field optics, the characteristics usually of greatest concern are the shape of the beam pattern, the flux concentration, and the dependence of the shape and signal on wavelength. We have tested heat traps for these characteristics using the configurations shown in Table I.

A. Beam Patterns

Ideally a field optics system should accept with unit efficiency all rays within the image space of the telescope; that is, all $\theta \leq \theta_1 = \arcsin(1/2f_T)$. The actual beam patterns of the three prototype heat traps (Table I) have been presented in Fig. 2.

The shape of the beam pattern is found to depend critically on the precision with which the collector surface is figured. At all points errors in collector radius, r, must be $<<\lambda$ and $<< r_2$, and errors in dr/dz must be $<< r_2/Z$ where Z is measured from the exit aperture. For the collectors used in these tests the radius was held within 0.025 mm at all values of z and within ~0.012 mm for all z within $\ell_L/20$ of the exit aperture.

The beam pattern also depends on the configuration of the cavity, but for the design described in sections IIIB and IIIC the relationships (21) to (24) the curves of Fig. 8 give an adequate indication of the required precision.

B. Flux Concentration

The flux concentration produced by a system of field optics may be determined by comparing the signal, I, with the field optics in place to the signal,

I_o, with the field optics removed. The ratio I/I_o is naturally compared with ratio of the areas of the entrance and exit pupils of the field optics. Typically I/I_o falls below $(r_1/r_2)^2$ by 20% - 30% for a moderately good system. Three factors which we shall call a, b, and c may contribute to this difference. Thus

$$I/I_o = a\ b\ c\ (r_1/r_2)^2. \tag{25}$$

The first factor, a, is necessary to allow for the practical difficulty of eliminating all reflections from surfaces inside the dewar, which may cause stray radiation to reach the bolometer. This effect tends to reduce the measured value of I/I_o since the "bare" bolometer necessarily has a wider angular acceptance than the field optics (i.e. $a < 1$ and hard to estimate).

The second factor, b, gives the transmission of the field optics. This factor is necessarily less than one. For ideal light collectors, however, it should be close to one, except perhaps for wavelengths comparable to r_2.

The third factor, c, allows for the increase in the effective absorptivity of the bolometer due to the cavity. This effect will increase both I and I_o, but if the cavity is matched to the field optics one expects a greater increase for I. Hence we expect $c > 1$.

Our measured value of the signal amplification for a heat trap matched to $f_T = 5$ ($\theta_1 = 5.7^\circ$) is $I/I_o = 108 \pm 10$. This may be compared with the geometrical ratio $(r_1/r_2)^2 = (f_T/f_F)^2 = 100$ ($f_F = 1/2$ for heat trap). Hence $abc \approx 1.1$. The measured value, 108 ± 10, may also be compared with the value 25 which could be achieved using a 100% efficient $f_F = 1$ system of the same angular acceptance (assuming $a = 1$).

The measured value of I/I_o refers to $\theta = 0^\circ$ only; it does not reflect the consequences of the heat trap's relatively favorable beam pattern. For an overall comparison of the signal amplification of the heat trap with that of more conventional systems (independent of the factor a) see section IVD.

C. Dependence on Wavelength

For the heat trap (f/0.5) expression (13) becomes

$$K\lambda \leq d_2 \leq 1.22\lambda. \qquad (26)$$

To test whether the heat trap satisfies this condition we have exposed each of two heat traps (d_2 = 1.0 mm and d_2 = 0.30 mm) to radiation of different wavelengths. Comparing the signals from the two systems, we find that there is no loss of efficiency between $\lambda/d_2 = 0.28$ (K = 3.6) and $\lambda/d_2 = 0.54$ (K = 1.85). Between $\lambda/d_2 = 0.9$ (K = 1.1) and $\lambda/d_2 = 1.7$ (K = 0.6) there is a loss of approximately 20%. Between $\lambda/d_2 = 1.7$ and $\lambda/d_2 = 3.3$ (K = 0.3) the loss is nearly 100%. Hence the signal amplification remains nearly constant up to wavelengths which are comparable to the exit aperture. We note that the calculations of Levine and Schwinger[9] for diffraction of scalar plane waves by apertures in infinite plane screens indicate an abrupt drop in transmission at about $\lambda/d = 1.8$. As shown in Fig. 9 there is little degradation of beam patterns out to values of λ/d_2 as large as 1.7.

We conclude that the interval defined by expression (26) does exist and hence that heat traps can produce maximum flux concentration without loss of resolution.

D. Observational Tests

In addition to the laboratory tests described above, we have made observational tests at two telescopes. One set of observations was conducted with the NASA 91-cm. airborne telescope of the Ames Research Center[10] using a heat trap with a 2' field of view (f_T = 13) and a filter with a low-pass cut-on of ~100μm. The other set of observations was conducted at the 200-inch Hale telescope at Mt. Palomar using a heat trap with a 3' field of view (f_T = 4) operated in the 1 mm atmospheric window.

Several factors must be considered when the observational tests with the heat trap are compared to those with other systems. These include

i) Aperture In addition to the geometrical factor which must be applied to signals obtained from extended sources the larger aperture of the heat trap will increase the wavelength at which the system is diffraction limited and may thus affect the bandpass of the observations.

ii) Beam Pattern The observed signals depend not only upon the efficiency for on-axis rays but also upon the angular dependence of the efficiency. For example the relatively flat-topped beam pattern of the f_T = 13 heat trap makes better use of marginal rays than the comparison system (an off-axis mirror system).

iii) Detector Corrections must be applied for differences in responsivity, absorptivity, and frequency response.

The corrections which must be applied reduce the accuracy of comparisons between systems and also make it difficult to attribute differences in overall

performance to particular characteristics of the field optics (e.g. the beam pattern or the effect of the cavity on absorptivity).

Nevertheless several general observations can be made about the performance of the heat trap. First, in both the f_T = 13 and f_T = 4 systems, the observed widths, θ_b, of the telescope beam patterns at the half-intensity points were close to the calculated values (see Fig. 9). Second, the telescope beam patterns were relatively flat-topped. And finally, the f_T/13 heat trap (which had a bolometer similar in size, speed, and electrical characteristics to that of the f1, 1' field of view comparison system) was apparently more efficient than the comparison system by a factor of about two (i.e. signals were twice as large for point sources).

Photometric data were obtained with the f_T = 4 heat trap at the 200-inch telescope. These are presented in Table II. The relative fluxes are consistent with those obtained with a lens system of one arc min beam at the same wavelengths.[11] The noise equivalent flux density of the system was approximately 100 Jy (normalized to 1 second integration time at 1.4 mm) for observations through ~1.4 air masses under atmospheric conditions such that the extinction was ~1.8 mag./air mass. The noise equivalent power of the bolometer used for these tests was significantly higher than for the best which are currently available.

The observations appear to be consistent with the results of the laboratory tests. We conclude that in observations of extended sources the heat trap is superior to conventional field optics systems. For point objects it is comparable.

Acknowledgements

We thank P.K. Kloeppel, J. Morris, C. Telesco, R. Treitel, and S. Whitcomb for assistance in various parts of this work.

We thank M. Werner for arranging and collaborating in the observational tests of the 7.2° heat trap at the Hale 200" telescope. We are grateful to L.H. Cheung for preparing the bolometer used in those tests and to F.J. Low and A.W. Davidson for the bolometers used in the laboratory tests.

We appreciate the assistance of the Ames Research Center staff throughout the airbone tests and of the Hale Observatories staff during the ground-based tests. We also appreciate the opportunity for one of us (RHH) to work as a Guest Investigator during the observations at Mt. Palomar.

We acknowledge with thanks support from the Luis Block Fund during the initiation of the work, from the Alfred P. Sloan Foundation for continued development and ground based tests, from the Energy Research and Development Administration [E(11-1)2594] for fabrication of prototype light collectors, and from the National Aeronautics and Space Administration (Grant No. NSG-2057) for the airborne tests.

REFERENCES

1. H. Hinterberger and R. Winston, Rev. Sci. Instr. 37, 1094 (1966).

2. V. K. Baranov and G. K. Mel'nikov, Soviet Journal of Optical Technology 33, 408 (1966).

3. Roland Winston, J. Opt. Soc. Am. 60, 245 (1970).

4. See, for example, M. Born, Principles of Optics 4th ed., Oxford, New York, Pergamon Press 1969.

5. Des Cartes, R., Oeuvres de Des Cartes, La Geometrie, Livre II (1637).

6. C. Huygens, Traite de la Lumiere, Le Hague, (1690).

7. E.N.K. Clarkson and Riccardo Levi-Setti, Nature, 254, 663 (1975), have shown that the trilobites employed Des Cartes and Huygens lens systems of about f = 1.1 as long as 600 million years ago.

8. H. Hinterberger and R. Winston, Rev. Sci. Instr. 39, 1217 (1968).

9. H. Levine and J. Schiwinger, Phys. Rev. 74, 958 (1948), and 75, 1423 (1949).

10. R. M. Cameron, M. Bader, and R. E. Mobley, Applied Optics 10, 2011 (1971).

11. M. W. Werner, Private Communication.

Table I Dimensions of Heat Traps Used in Performance Tests

	θ_1		
	7.18°	5.74°	2.20°
f_T	4	5	13
d_1 (mm)	18	10.16	8.58
d_2 (mm)	2.25	1.016	0.330
ℓ_L (mm)	80.35	55.60	115.74
d_C (mm)	4.0	1.6	0.80
ℓ_C (mm)	4.0	1.6	0.80
ℓ_B (mm)	1.46	0.56	0.30
ℓ_B/ℓ_C	0.37	0.35	0.37
a_B[a] $(mm)^2$	2.4 X 2.4	$\pi(0.6)^2$	0.35 X 0.35
w[b] (mm)	0.8	0.35	0.25
C[c]	64	100	676

[a] a_B = cross section of bolometer

[b] w = width of slot for bolometer leads

[c] $C = (d_1/d_2)^2 = (2f_T)^2$ = concentration factor

Table II Signals from Sources Observed at the 200-Inch Hale Telescope Using the 7.2° Heat Trap

Source	Date (1975)	Signal (Jy)[a]
Mars	May 24	191 ± 13
Jupiter	May 24	4190
W51	May 24	102 ± 9
K3-50	May 24	17 ± 5
W49	May 22	119 ± 13

a The relative signals have been corrected for atmospheric absorption and normalized such that the Jupiter signal has the flux density expected at λ = 1.4 mm for a 150°K black body subtending the solid angle of the planet (semi diameter 16.4 arc sec).

FIGURE CAPTIONS

Fig. 1 Heat Trap (Schematic)

The parabola P (axis A and focus F) is rotated about the optic axis, Z, to generate the collector surface. The surface is parallel to Z at the entrance aperture. The angle θ_1, between A and Z is equal to the cut-off angle for entering rays. The collector is drawn for $\theta_1 = 10^\circ$ corresponding to a telescope focal ratio $f_T = 2.88$.

Fig. 2 Observed (solid line) and calculated (dashed line) infrared beam patterns for three heat traps with cylindrical cavities (Table I). The calculated curves take into account the inherent acceptance of the collectors (Fig. 5), diffraction at the entrance apertures, losses at each reflection, and the finite apertures of the test source and collectors. The arrows indicate the nominal cut-off angles, θ_1.

Fig. 3 Idealized configuration of field optics employing a concave mirror and on-axis detector. A. Disc-shaped detector. B. Spherical detector.

Fig. 4 Observed infrared beam pattern for a 7.2° heat trap with a hemispherical cavity (See inset Fig. 7).

Fig. 5 Angular cut-off interval of an ideal light collector calculated for a point source at infinity with $\lambda << d_2$. The quantity $\Delta\theta$ is the angular interval in which the intensity drops from 3/4 to 1/4 of its maximum value (see inset).

Fig. 6 Optical model (schematic). The entrance aperture of the model heat trap is exposed to uniform illumination from the inside surfaces of the white box. The light reflected at angle θ is measured by the photocell.

Fig. 7 Beam patterns obtained with the optical model (reflected light). The bottom curve was obtained with the exit aperture of the light collector opening into a dark room. The top curve was obtained with a hemispherical cavity (inset) of proportions $d_B = 1.2\ d_2$ and $r_C = 3.3\ d_2$ with the bolometer surface below the aperture by $d_2/2$. The solid-line curves were obtained with a gray bolometer in a cylindrical cavity of proportions $d_B = d_2$ and $d_C = \ell_C = 2d_B$, at various values of ℓ_B/ℓ_C (symbols defined in Fig. 1).

Fig. 8 Beam patterns of a 2.2° heat trap of exit diameter $d_2 = 330\mu m$ at wavelengths $\lambda = 280\mu m$ (solid line) and $\lambda = 550\mu m$ (dashed line). (The solid angle of the source was larger than that used for Fig. 2A).

Fig. 9 Scan of Jupiter at the Hale 200-inch telescope using the 7.2° heat trap. The calculated field of view has a diameter of 3.05 arc min. The lower portion of the figure shows, for comparison, the convolution of a 3.05 arc min aperture with the diffraction pattern expected for a point source at a wavelength $\lambda = 1.4$ mm.

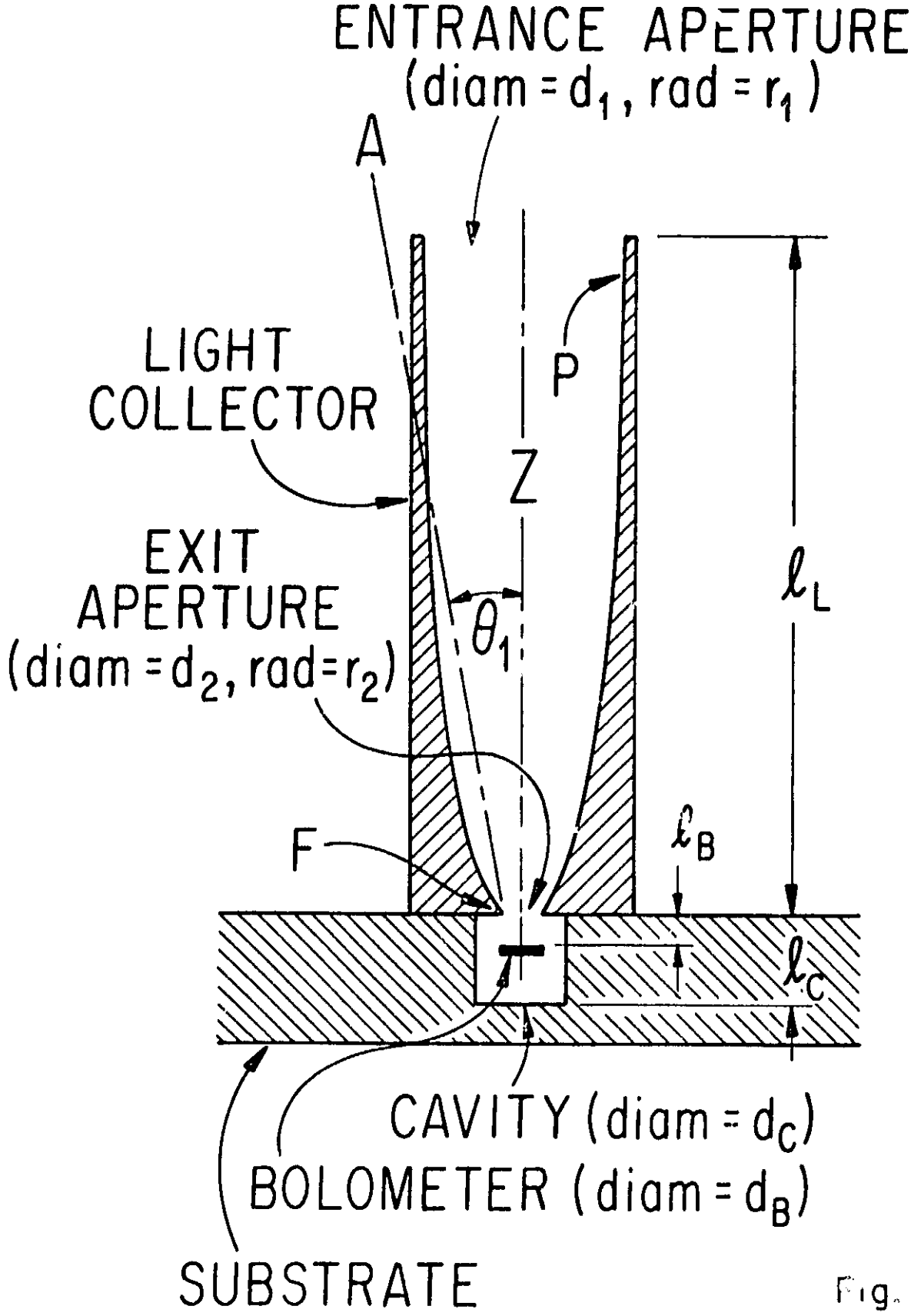
ENTRANCE APERTURE
(diam = d_1, rad = r_1)
A
LIGHT
COLLECTOR
P
Z
EXIT
APERTURE
(diam = d_2, rad = r_2)
θ_1
ℓ_L
F
ℓ_B
ℓ_C
CAVITY (diam = d_C)
BOLOMETER (diam = d_B)
SUBSTRATE

Fig. 1

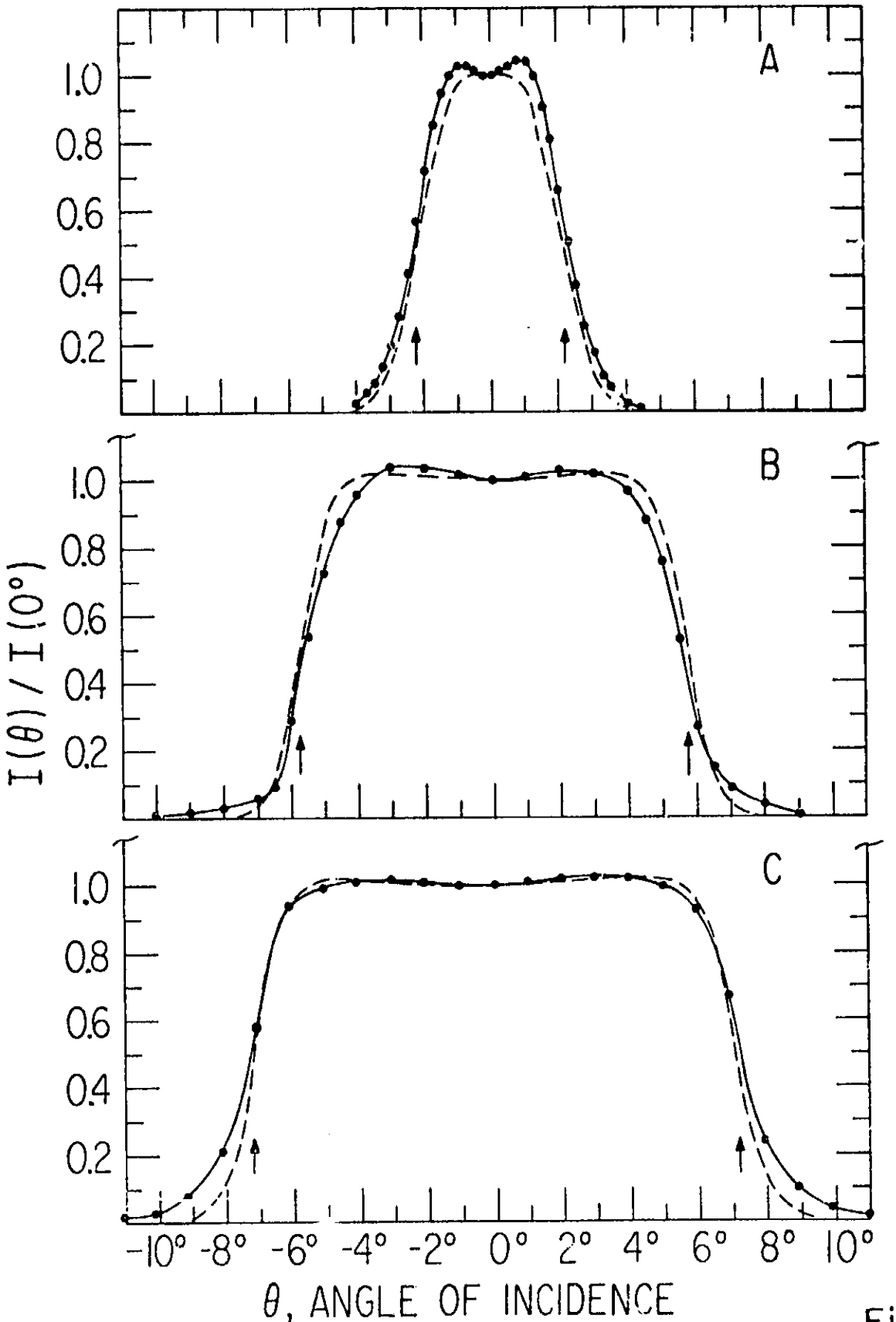

Fig.2

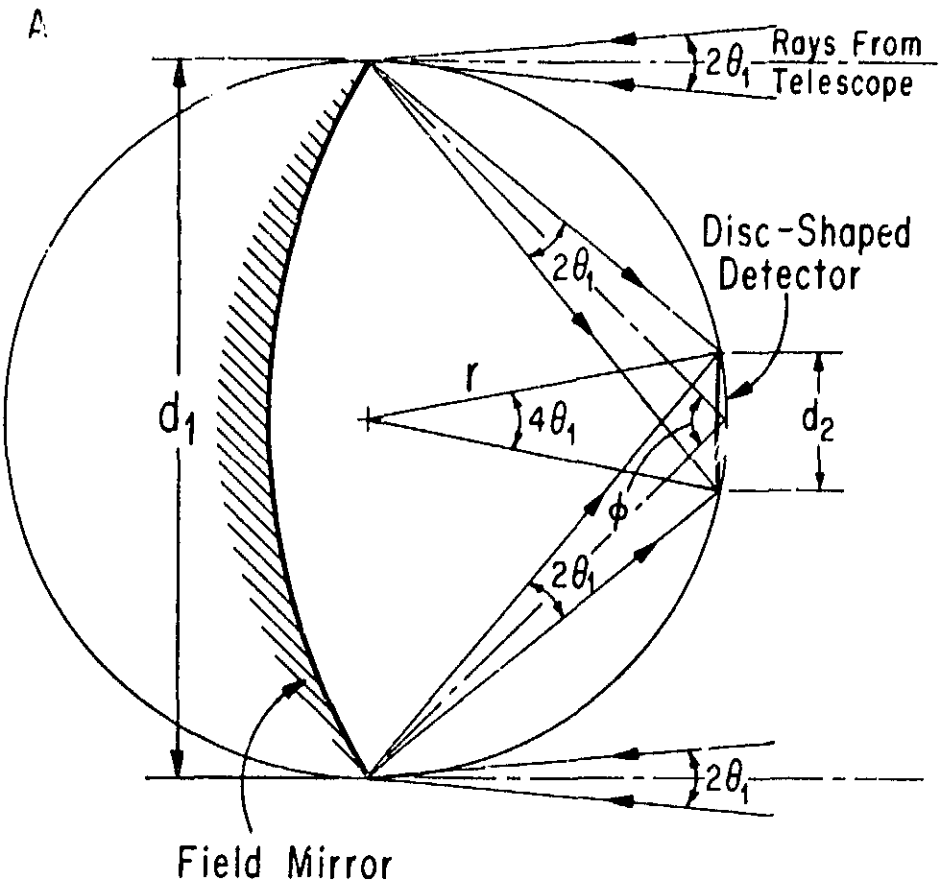

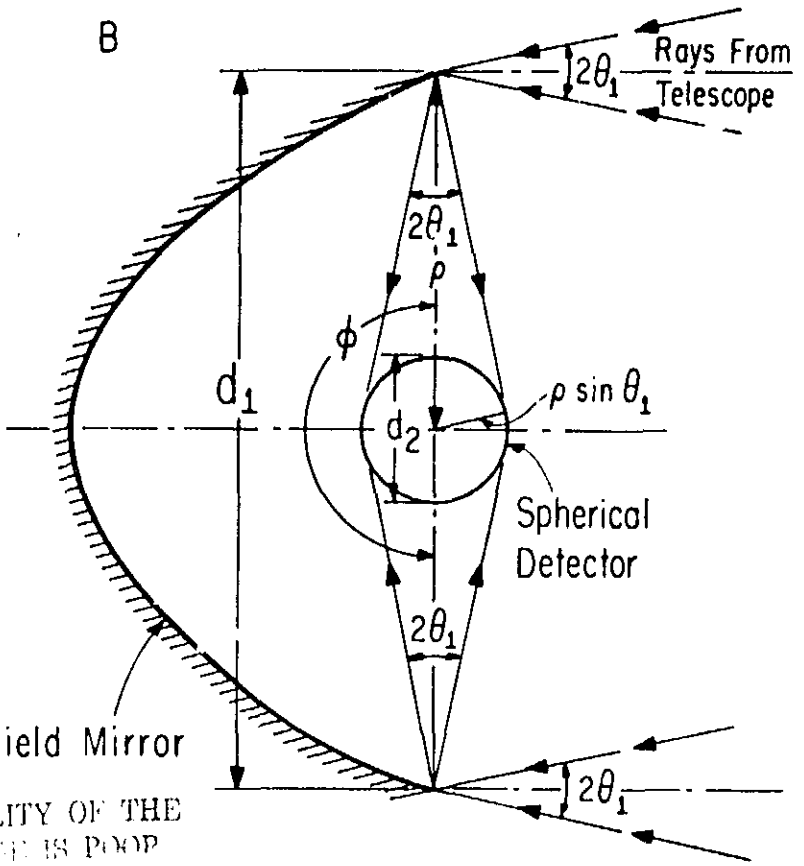

Fig.3

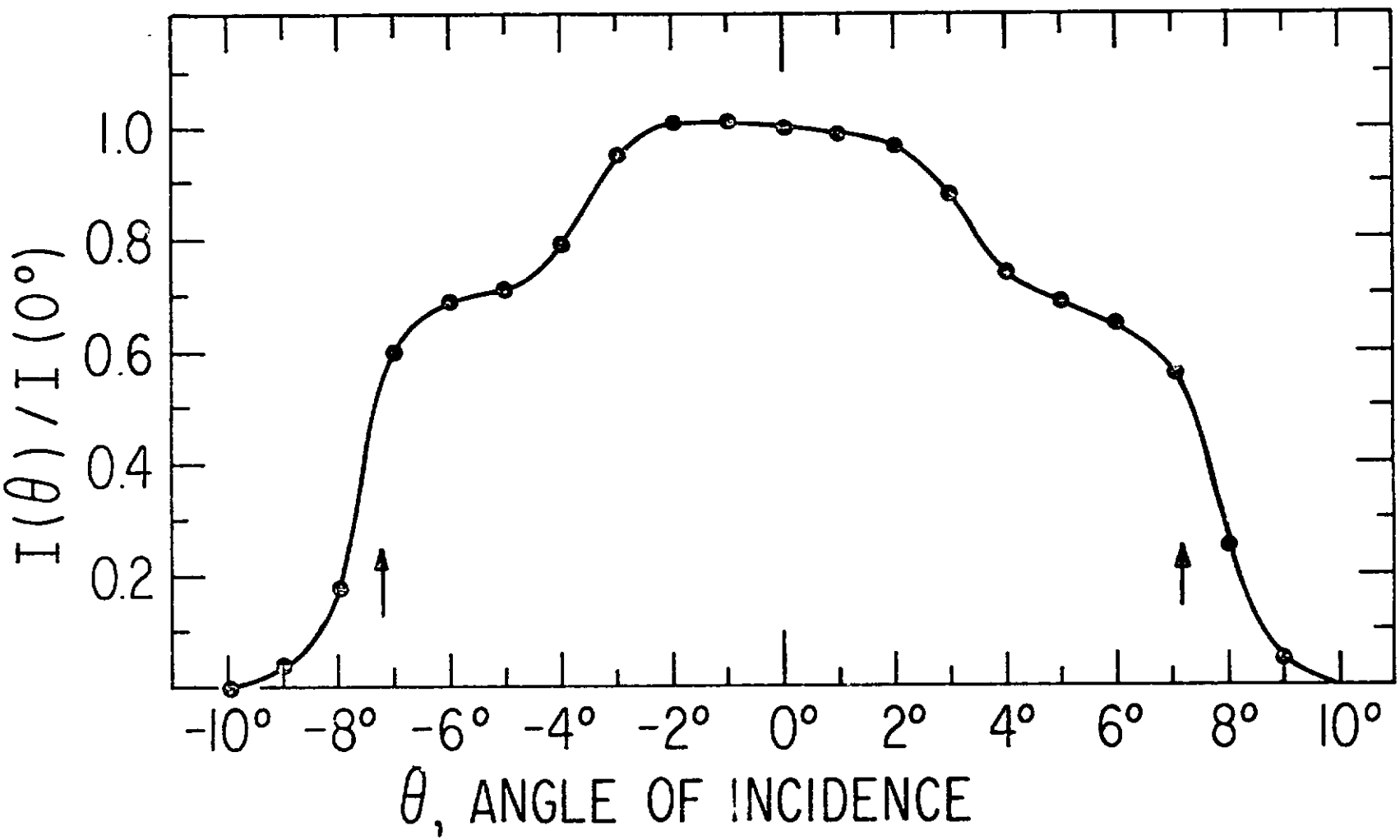

Fig.4

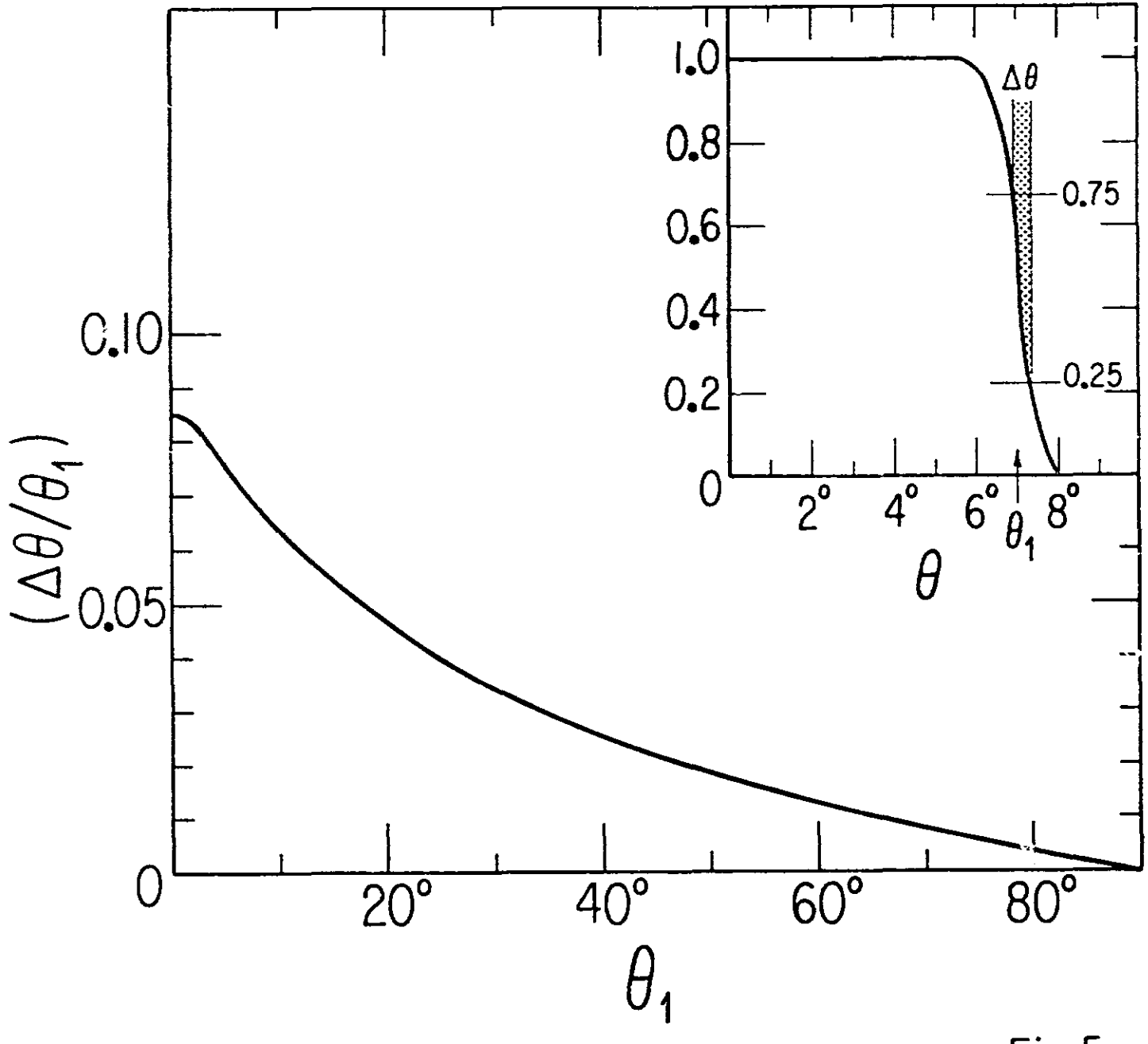
0.10
0.05
0
$(\Delta\theta/\theta_1)$
20°
40°
60°
80°
θ_1
1.0
0.8
0.6
0.4
0.2
0
$\Delta\theta$
0.75
0.25
2°
4°
6°
θ_1
8°
θ

Fig.5

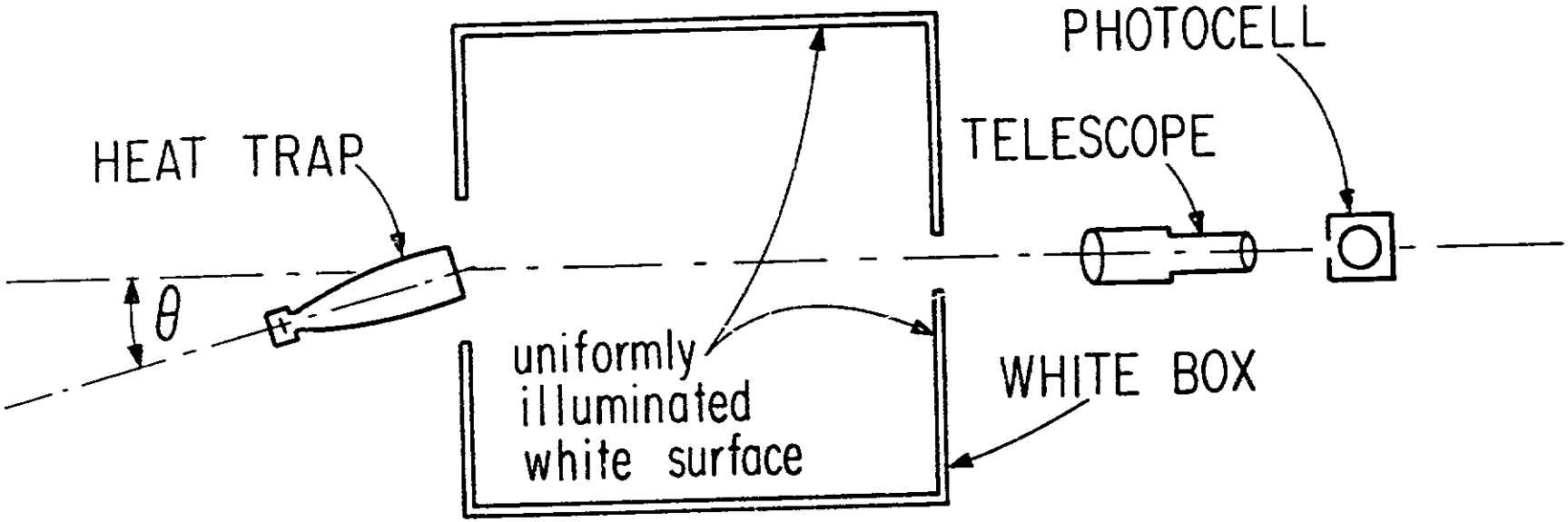
PHOTOCELL
HEAT TRAP
TELESCOPE
θ
uniformly
illuminated
white surface
WHITE BOX

Fig.6

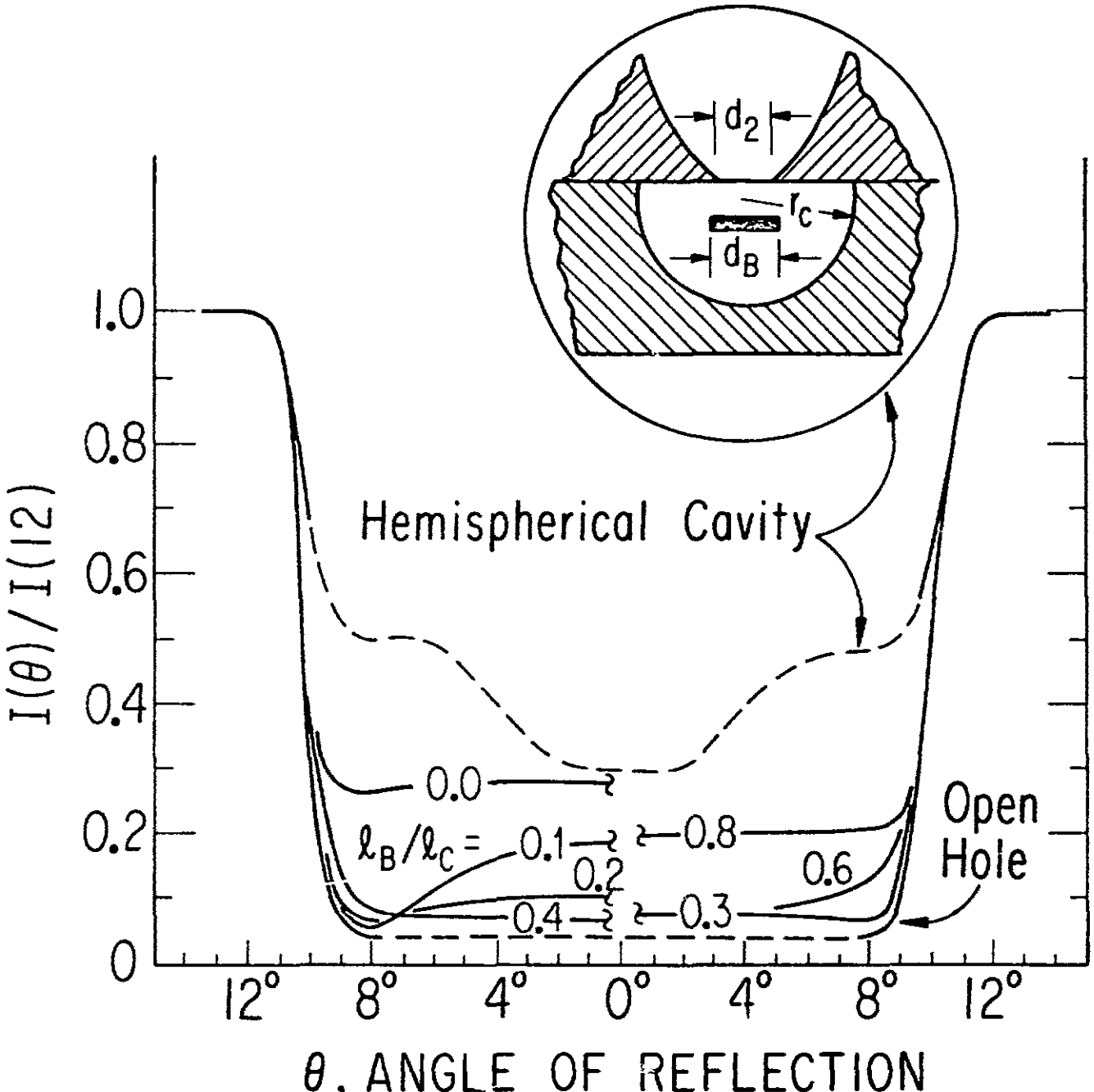
d_2
r_c
d_B
Hemispherical Cavity
1.0
0.8
0.6
0.4
0.2
0
$I(\theta)/I(12)$
0.0
ℓ_B/ℓ_C = 0.1
0.2
0.4
0.8
0.6
0.3
Open Hole
12°
8°
4°
0°
4°
8°
12°
θ, ANGLE OF REFLECTION

Fig.7

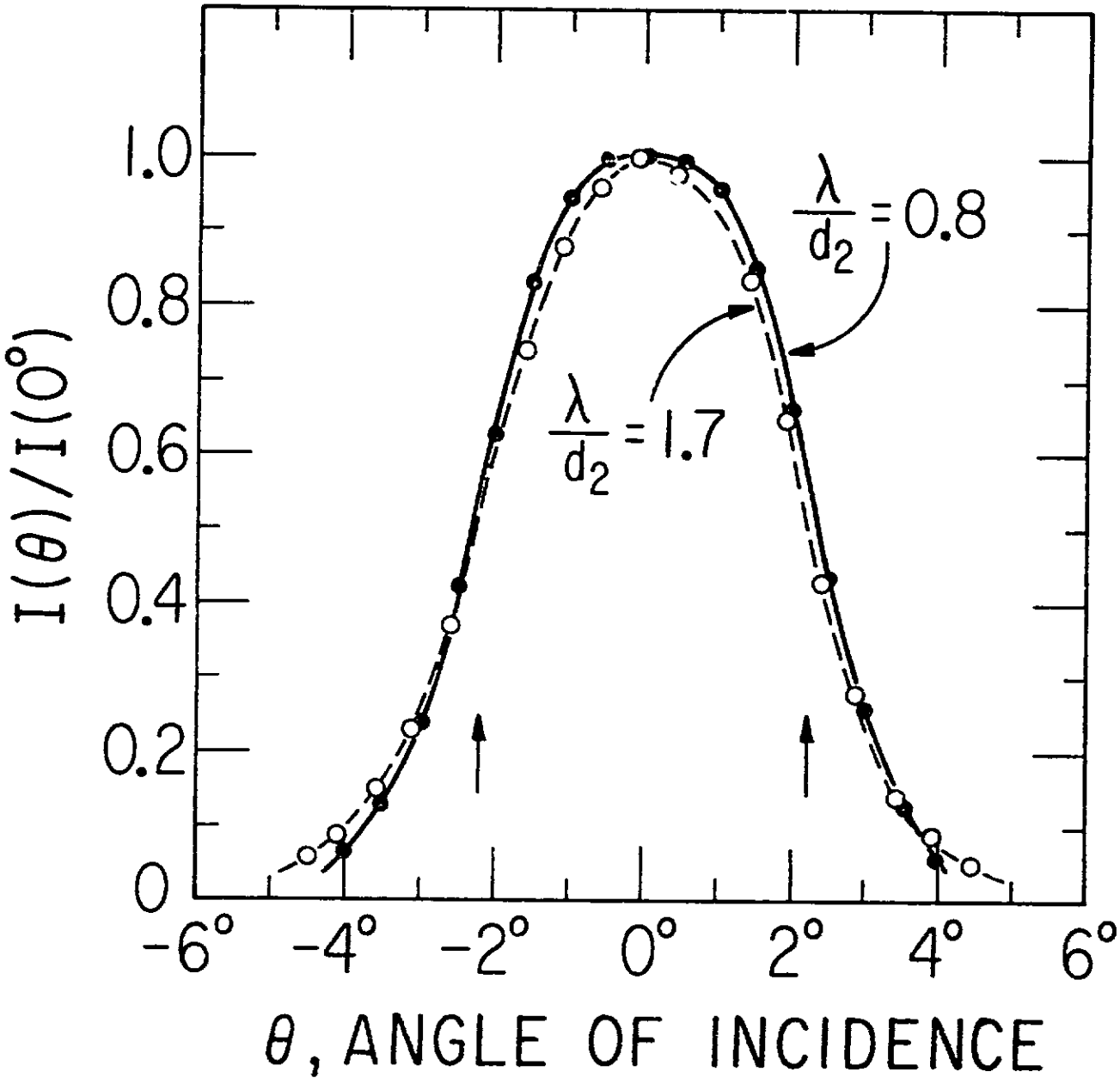

Fig.8

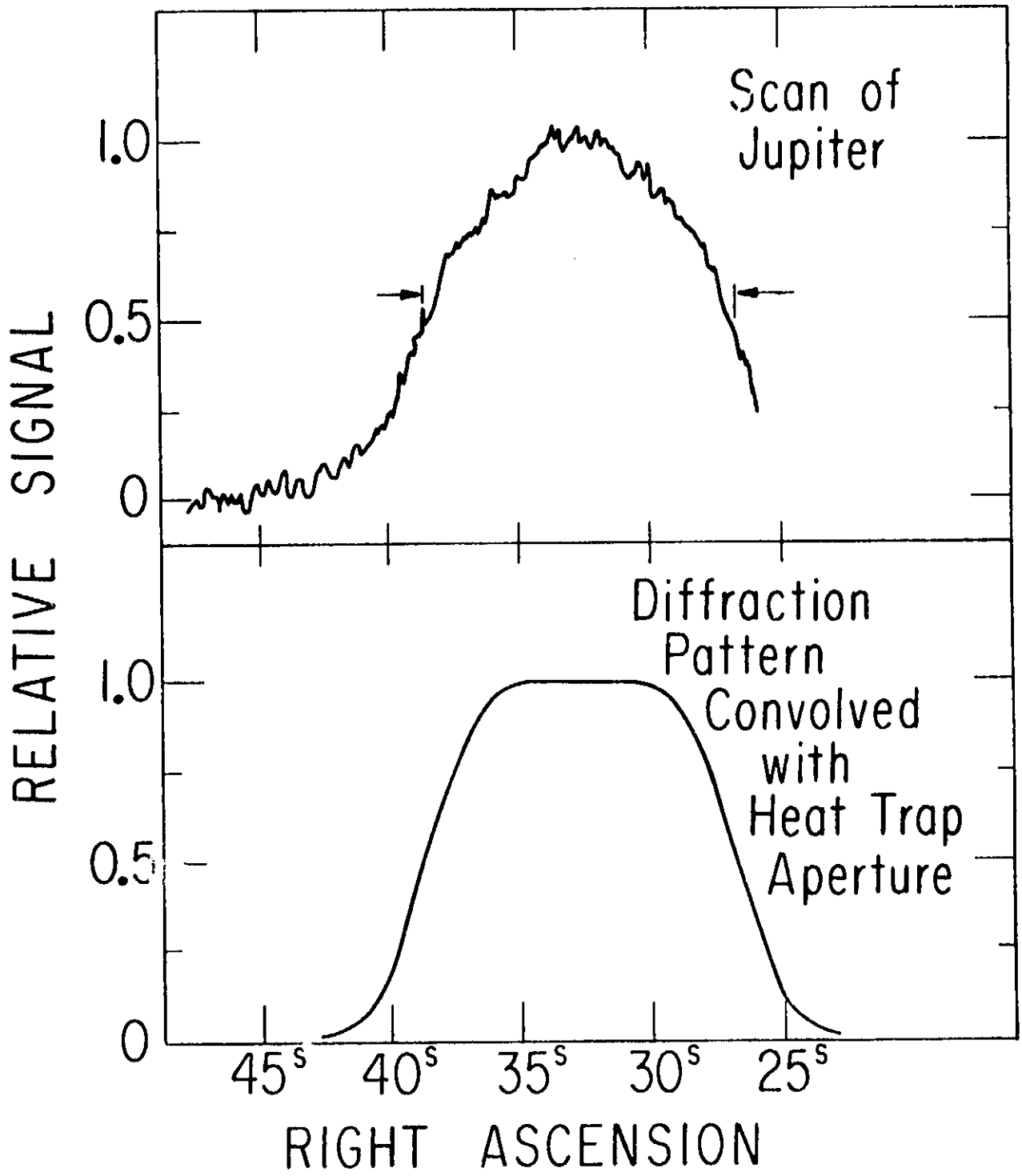
Scan of Jupiter
1.0
0.5
0
Diffraction Pattern Convolved with Heat Trap Aperture
1.0
0.5
0
RELATIVE SIGNAL
45s
40s
35s
30s
25s
RIGHT ASCENSION

Fig. 9